ELSEVIER

Biophysical Chemistry 84 (2000) 77–85

Biophysical Chemistry

www.elsevier.nl/locate/bpc

Thermodynamical model of mixed aggregation of ligands with caffeine in aqueous solution. Part II ☆

Malgorzata Zdunek[a], Jacek Piosik[a], Jan Kapuscinski[b,*]

[a] *University of Gdansk, 80-222 Gdansk, Poland*
[b] *Department of Molecular and Cellular Biology, Intercollegiate Faculty of Biotechnology, University of Gdansk and Medical University of Gdansk, 80-822 Gdansk, Poland*

Received 9 August 1999; accepted 7 December 1999

Abstract

A statistical–thermodynamical model of mixed association in which one component's self-association is unlimited while the second component does not self-aggregate is described. The model was tested with 4′,6-diamidino-2-phenylindole-dihydrochloride (DAPI) and ethidium bromide (EB) using light absorption spectroscopy and calorimetry. The system is controlled by two parameters, which represent self-aggregation 'neighborhood' association constant K_{CC} and mixed 'neighborhood' association constant K_{AC}. Calculated, using this model, $K_{AC} = 58.2 \pm 1\ M^{-1}$, $K_{AC} = 64.6 \pm 2\ M^{-1}$ for DAPI and EB, respectively, are in good agreement with known values of stacking interactions. The titration microcalorimetric measurement of DAPI–CAF interaction $\Delta H = -11.1 \pm 0.4$ kcal/mol is also consistent with this type of reaction. The structures of the stacking complexes were also confirmed by semi-empirical molecular modeling in the presence of water. The data indicate that CAF forms stacking complexes with DAPI and EB, thus effectively lowering the concentration of the free ligands in the solution, and therefore, CAF can be used to modulate aromatic compound activity.

Keywords: Caffeine; DAPI; Ethidium bromide; Light absorption spectroscopy; Calorimeter; Molecular modeling; Stacking interactions

* Corresponding author.
☆ Part I: J. Kapuscinski and M. Kimmel, Biophys. Chem. 46 (1993) 153.

0301-4622/00/$ - see front matter
PII: S0301-4622(99)00152-0

1. Introduction

Caffeine (CAF, Fig. 1) is a chemical well known for its capacity to enhance the lethal effect of some DNA-damaging agents such as ionizing radiation [1], alkylating compounds [2], cisplatinium [3–5], cyclophosphamid [6] and hydroxyurea [7]. In contrast, however, the cytotoxic and cytostatic activity of aromatic, antitumor agents such as camptothecin or topotecan [8] and ellipticine or mitoxantrone [9], which are the topoisomerase I and II blockers, are diminished in the presence of CAF. It also reduces the toxicity of ethidium bromide [10]. Lately, we have obtained evidence that CAF inhibits cytogenic activity of quinacrine mustard but not mechlorethamine (Kapuscinski et al., unpublished data). The protective effect of CAF is most likely due to formation of complexes between CAF and these aromatic molecules, which result in a reduction of the effective concentration of the free form of drugs available to the cells. While formation of such complexes between CAF and some aromatics has already been demonstrated, there was no model to enable one to calculate ligand concentration in its mixture with CAF, when ligand does not aggregate. There were two statistical–thermodynamical models of indefinite mixed association developed. In one, developed by Weller et al. [11], both components, CAF and ligand, can form indefinite stacks. In Kapuscinski–Kimmel's model [12], aggregation of the ligand is limited to dimerization only. In our system, however, ligand does not aggregate in solutions in which its concentration is in the micromolar (μM) range [13]. The aim of this study was to create the statistical–thermodynamical model which would allow one calculate the concentration of any component present in the mixture and association constant. To test the created model two non-aggregating, DNA-binding chemicals were chosen. EB (Fig. 1), which is an intercalator [14–16] and DAPI (Fig. 1), which has two modes of the binding: intercalative and minor-groove binding [13].

2. Materials and methods

Caffeine (CAF), 4′,6-diamidino-2-phenylindole-dihydrochloride (DAPI) and ethidium bromide (EB) were purchased from Sigma (St. Louis, MO, USA). CAFs stock solution was prepared by dissolving the weight amount in HP buffer. HP buffer contains 5 mM Hepes (*N*-[2-hydroxyethyl]-piperazine-*N*′-[2-ethanesulfonic acid]) at 0.1 M NaCl and pH 7.1.

DAPI and EB were dissolved in distilled water as the stock solutions followed by further dilutions in HP buffer. The concentrations of solutions were assayed colorimetrically using molar absorption coefficients of $E_{340} = 2.7 \times 10^4$ M^{-1} cm^{-1} and $E_{480} = 5.85 \times 10^3$ M^{-1} cm^{-1} for DAPI and EB, respectively. All experiments were performed in the HP buffer at 25 ($\pm$0.1) °C. The buffers were filtered through a 0.45-μm pore Millex Millipore filter and then degassed by helium.

Light absorption spectra were measured using Beckman's DU 650 spectrophotometer thermostated with Polystat's temperature constant

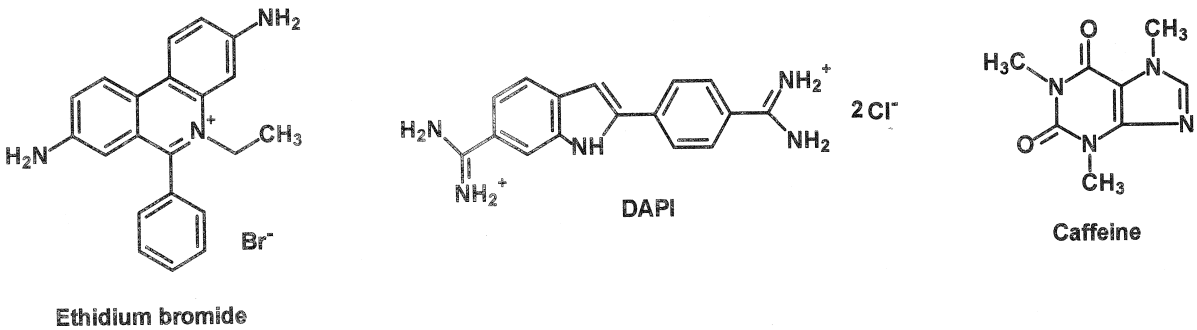

Fig. 1. Chemical structures of ethidium bromide, DAPI and caffeine.

circulator. The 2-ml aliquot containing ligand were placed in a quartz cuvette (1 cm light path) to the spectrophotometer and titrated with CAF dissolved in the buffer. The absorption spectra were then measured at 1-nm intervals and stored in digital form. The spectra were corrected for the absorption of the buffer and CAF, which were very low in the measured range, and then expressed in the form of molar absorption coefficient (E_λ M^{-1} cm^{-1}).

The heat of DAPI–CAF interaction was measured using an Omega Microcalorimeter. Ten portions of the titrant, 10 μl each, were added to 1.3 ml of the titrated solution and the heat of the process was measured as a function of time (μ cal/s). Data such as these were corrected for ligand and CAF heats of dilution, processed on the computer, and then deconvoluted using an algorithm based on the Marqardt–Levenberg method, which allowed us to estimate heat of complex formation.

Molecular modeling was performed using HyperChem, Hypercube Inc. software. We used a semi-empirical method (PM3) allowing one to calculate electronic properties, optimized geometries and total energy [17]. We used the geometry optimization method to find a minimum-energy (stable) configuration for the molecular system, these calculations adjust atomic coordinates in steps to find a configuration in which net forces on each atom are reduced to zero; this is usually a local minimum on the potential surface. To take into consideration hydrophobic and hydrophilic forces, we 'put' our molecular system into a periodic box containing molecules of water; these periodic boundary conditions simulate a continuous system with a constant density of molecules.

3. Results and discussion

In our model we follow the notation and definition used by Weller et al. [11]. There are two types of molecules in our system: A (e.g. DAPI) and C (e.g. CAF). Relative concentrations of the components are calculated using the partition function Z of the system. This function is obtained by adding the statistical weights of all the states accessible to all types of oligomers. Thus, the statistical weight of any oligomer contains: (i) a factor C_A for each A; (ii) a factor C_C for each C; (iii) the factors K_{CC} and C_{CC} for each CC neighborhood; and (iv) the factors K_{AC} and C_{AC} for each AC neighborhood. C_C and C_A are the concentrations of isolated (i.e. free) A and isolated C molecules in solution, C_{CC} and C_{AC} are the CC and AC neighborhood concentrations, respectively, and K_{CC} and K_{AC} denote the nearest neighbor equilibrium constants of association of C with C and A with C, respectively. Molecules can form different self- and mixed-aggregates of a type:

$$\ldots(C)_i(A)_j(C)_i(A)_j\ldots, \quad \text{where } i = 0,1,2\ldots \text{ and } j = 0,1.$$

If component A may form an aggregate of the length at least of $j = 1$ only, therefore, the partition function is equal to:

$$Z = C_A + \sum_{i \geq 1} C_{C,i} \tag{1}$$

where;

$$C_{C,i} = K_{CC}^{i-1} \cdot C_C^i \cdot (1 + K_{AC} \cdot C_A)^2 \times \left[1 + \frac{K_{AC}^2}{K_{CC}} \cdot C_A\right]^{i-1} \tag{2}$$

After calculating the sum of the infinite geometric progression,

$$Z = C_A + \frac{C_C \cdot (1 + K_{AC} \cdot C_A)^2}{1 - C_C \cdot (K_{CC} + K_{AC}^2 \cdot C_A)} \tag{3}$$

The total concentrations of A and C can be obtained as,

$$C_{TA} = C_A \cdot \frac{\partial Z}{\partial C_A} = C_A \cdot \left[\frac{1 - C_C \cdot (K_{CC} - K_{AC})}{1 - C_C \cdot (K_{CC} + K_{AC}^2 \cdot C_A)}\right]^2 \tag{4}$$

$$C_{TC} = C_C \cdot \frac{\partial Z}{\partial C_C}$$

$$= C_C \cdot \left[\frac{1 + K_{AC} \cdot C_A}{1 - C_C \cdot (K_{CC} + K_{AC}^2 \cdot C_A)} \right]^2 \quad (5)$$

In a similar way it is possible to obtain concentrations of neighborhoods CC and AC using the partition function:

$$C_{AC} = K_{AC} \cdot \frac{\partial Z}{\partial K_{AC}}$$

$$= 2 \cdot K_{AC} \cdot C_A \cdot C_C \cdot (1 + K_{AC} \cdot C_A) \times \frac{1 - C_C \cdot (K_{CC} - K_{AC})}{\left[1 - C_C \cdot (K_{CC} + K_{AC}^2 \cdot C_A)\right]^2} \quad (6)$$

$$C_{CC} = K_{CC} \cdot \frac{\partial Z}{\partial K_{CC}}$$

$$= K_{CC} \cdot \left[\frac{C_C \cdot (1 + K_{AC} \cdot C_A)}{1 - C_C \cdot (K_{CC} + K_{AC}^2 \cdot C_A)} \right]^2 \quad (7)$$

To check if the model is correct; we put $K_{AA} = 0$, (A molecule does not self-aggregate, so the nearest neighbor equilibrium constant of association of A with A is equal to zero) to the equation describing partition function in Weller's model and we obtained Eq. (3) after some arrangements. We obtained the same equation after putting $K_{AA} = 0$ to the Kapuściński–Kimmel's partition function equation. These calculations prove our model is correct.

Eqs. (4)–(7) enable one to calculate the unknown concentrations C_C, C_{CC}, C_{AC} and constant K_{AC}, with known K_{CC}, C_{TA} and C_{TC}. It should be pointed out that C_{CC} and C_{AC} are not concentrations of dimers CC and AC, respectively, but they count all neighborhoods in all possible oligomers. Based on mass conservation law molecular concentrations of A and C bound in mixed oligomers (X_{BA} and X_{BC}, respectively) can be calculated:

$$X_{BA} = C_{TA} - C_A \quad (8)$$

$$X_{BC} = C_{TC} - C_C - X_{CC} \quad (9)$$

where X_{CC} is molecular concentration of C self-aggregation:

$$X_{CC} = \frac{K_{CC} \cdot C_C^2}{1 - K_{CC} \cdot C_C} \cdot \left[2 + \frac{K_{CC} \cdot C_C}{1 - K_{CC} \cdot C_C} \right] \quad (10)$$

3.1. Spectroscopic measurements

The absorption spectra changes of DAPI titrated with CAF are presented in Fig. 2a. By extrapolation of $C_{TA}/C_{TC} \rightarrow 0$ the spectrum of the DAPI–CAF complex was calculated, where C_{TC} and C_{TA} are total concentrations of CAF and ligand, respectively. Observed complexes are the complexes of DAPI monomer with one or more CAF molecules. The range of wavelength has been chosen in such a way as to reflect only changes in the structure of DAPI, because CAF has neglectible light absorption over 350 nm. The presence of an isosbestic point in the spectra presented in Fig. 2a, indicates that only two components are present in the mixtures, most obvious being a monomer of DAPI and the DAPI–CAF complex. In a separate experiment we confirmed that DAPI and EB do not aggregate in the concentrations we used in our experiment (results not shown) [13,18]. The absorption spectra changes of EB titrated with CAF and the EB–CAF complex spectrum were measured too (Fig. 2b). There are changes in the electronic structure of EB and there are two components in the mixture: EB monomer and EB–CAF complex. It is indicated by the presence of an isosbestic point.

The spectra of ligand titrated with CAF, expressed as a molar absorption coefficient E_λ can be decomposed into a weighted sum of components by non-linear regression analysis, as previously described [12]. We used two-component (ligand monomer and ligand complexed with CAF) analysis of the mixtures. The examples of this procedure are shown in Fig. 3a,b. The spectra

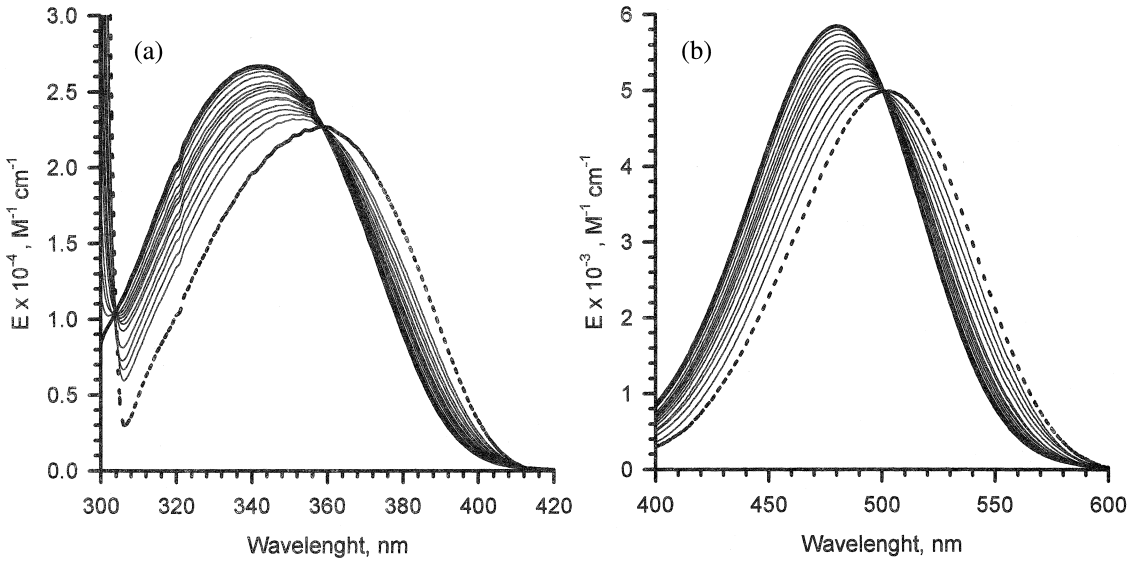

Fig. 2. Spectrophotometric titrations of ligands with caffeine. (a) Titration of DAPI (initial concentration 14.15 μM) with caffeine (0.26. ÷ 18.82 mM). Spectrum of free DAPI (—); extrapolated spectrum of DAPI–CAF complex (. . .). (b) Titration of ethidium bromide (initial concentration 68.61 μM) with caffeine (0.27 ÷ 14.38 mM). Spectrum of free EB (—); extrapolated spectrum of EB–CAF complex (. . .).

decomposition was made in the range of wavelength where standard errors have maximum values, and they were less then 0.01 in most cases. For this calculation we used the Marquardt–

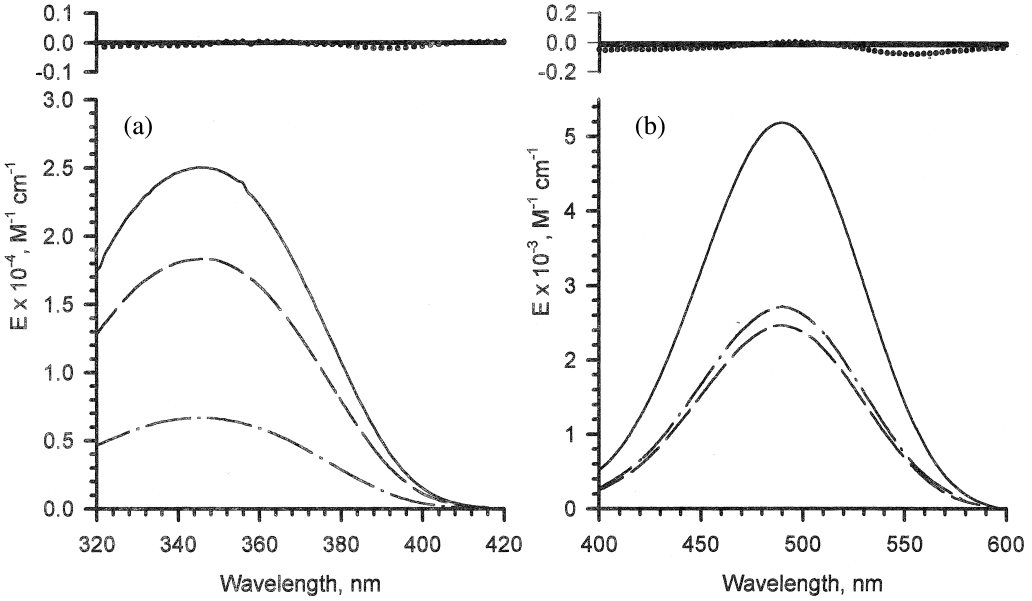

Fig. 3. Two-parameter analysis (decomposition) of DAPI–CAF and ethidium–CAF mixture. (a) Under the spectrum of mixture (—) DAPI (13.74 μM) with caffeine (2.99 mM), there are spectra of free DAPI (— —) and DAPI complexed with caffeine (— · —) scaled in proportion to their molar fraction in the mixture (see table). (b) Similar decomposition of mixture ethidium (63.8 μM) with caffeine (7.69 mM).

Table 1
Titration of DAPI with caffeine in 0.1 M NaCl, 5 mM Hepes, pH 7.1 at 25°C[a]

Component total concentration		DAPI molar fraction		Component concentrations						Association constant
C_{TC} (mM)	C_{TA} (μM)	DAPI free	DAPI complexed	C_A (μM)	C_{A2} (μM)	C_C (mM)	C_{AC} (μM)	X_{BA2} (μM)	X_{CC2} (mM)	K_{AC} (M^{-1})
0.0	14.15	1.0	0.0	14.15	14.15	0.0	0.0	0.0	0.0	–
0.26	14.11	0.972	0.028	13.72	13.71	0.25	0.41	0.41	0.0	56.8
0.51	14.08	0.943	0.057	13.28	13.29	0.50	0.80	0.79	0.0	59.2
1 01	14.01	0.899	0.101	12.60	12.52	0.98	1.54	1.49	0.02	54.8
1 51	13.94	0.841	0.159	11.73	11.82	1.44	2.21	2.12	0.05	61.0
2.01	13.87	0.799	0.201	11.09	11.18	1.90	2.83	2.69	0.08	60.7
2.50	13.80	0.766	0.234	10.58	10.61	2.34	3.41	3.19	0.13	58.9
2.99	13.74	0.734	0.266	10.08	10.08	2.76	3.94	3.66	0.18	58.2
3.94	13.60	0.667	0.333	9.07	9.16	3.58	4.89	4.45	0.31	59.8
4.88	13.47	0.631	0.369	8.50	8.37	4.36	5.71	5.10	0.46	56.2
7.15	13.16	0.554	0.446	7.29	6.86	6.13	7.32	6.30	0.94	51.9
9.32	12.86	0.494	0.506	6.35	5.77	7.69	8.49	7.09	1.53	49.9
13.37	12.30	0.401	0.599	4.93	4.33	10.34	10.00	7.97	2.92	49.3
18.82	11.54	0.318	0.682	3.67	3.11	13.44	11.10	8.43	5.25	48.6
										Mean: 58.2 ± 1.2

[a]*Abbreviations*: C_{TC}, total CAF concentration; C_{TA}, total DAPI concentration; C_A, concentration of monomer DAPI (experimental); C_{A2}, concentration of monomer DAPI; C_C, concentration of monomer CAF; C_{AC}, concentration of neighborhoods DAPI-CAF complexes; X_{BA2}, concentration of DAPI–CAF complexes; X_{CC2}, concentration of CAF–CAF complexes; K_{AC}, association constant DAPI–CAF.

Levenberg algorithm-based SigmaPlot (Jandel Scientific, CA, USA) program.

For calculations we used the $K_{CC} = 11.3$ M^{-1} value reported by Fritzsche et al. [19], total con-

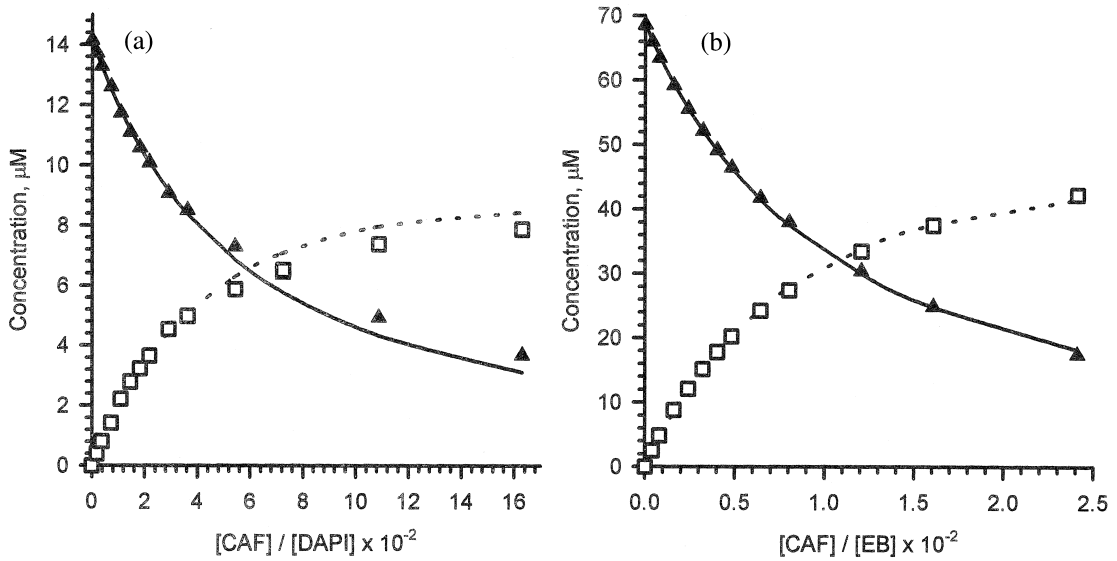

Fig. 4. The comparison of the results of two-parameter analysis of the mixtures DAPI with caffeine (a) and ethidium with caffeine (b) using measured and calculated data; (▲ and —) monomer of ligand; (□ and …) ligand complexed with caffeine.

centrations of ligands (C_{TA}), CAF (C_{TC}) and the measured free ligand concentration (C_A). K_{AC} was obtained using iteration program as described by Kapuscinski and Kimmel [12]. Having K_{AC}, all concentrations of neighbors can be calculated based on total component concentrations.

Based on the mass conservation law we were able to calculate molecular concentration of aggregated CAF (X_{CC}) and molecular concentration of AC complex (X_{BA}) (results given in Table 1).

The comparisons of the measured and calculated values are presented in Fig. 4a,b. There was good correlation between these data, in both cases, with S.E. not exceeding 0.5 μM for DAPI and 2 μM for EB.

EB is an intercalator and DAPI has been considered as a classical narrow-groove binder in terms of their fluorescent properties. We measured fluorescence spectra of these ligands titrated with CAF (results not shown), and the hyperchromicity was apparent in both cases. As CAF itself has very low fluorescence, obviously it may modify the ligand's fluorescence spectra upon binding; observed hyperchromicity followed complex formation with CAF.

4. Microcalorimetric titrations

We have also studied the interaction between CAF and DAPI by titration microcalorimetry.

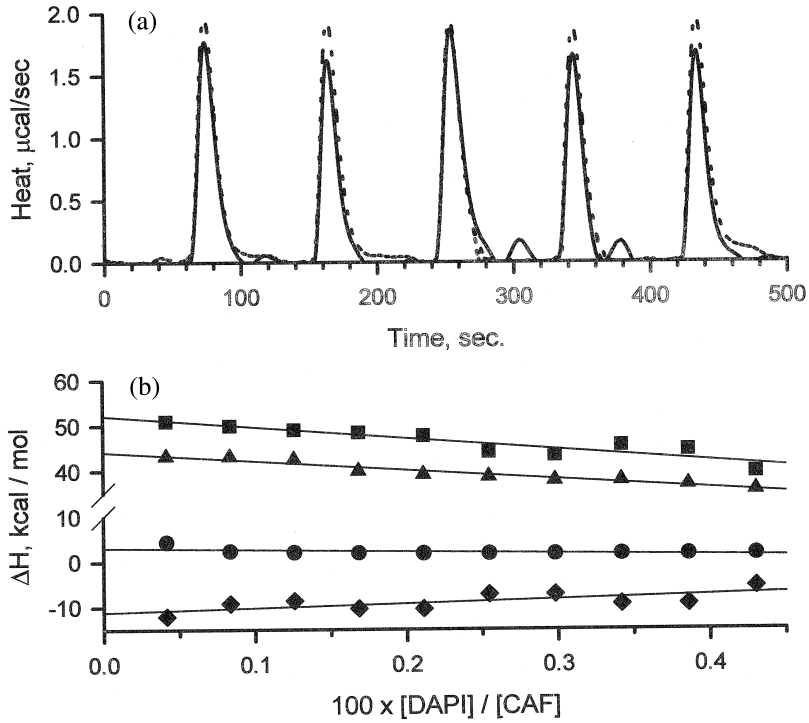

Fig. 5. (a) Microcalorimetric titration of CAF (1.33 ml at concentration 17.72 mM) with DAPI (1.27 mM) dissolved in HP buffer. Ten aliquots (10 μl each) of the titrant were added at 2-min intervals and the heat of exchange (μcal/s) measured as a function of time. CAF solution with buffer (---) and CAF solution with DAPI (—). For clarity of the picture only first five points of titration are shown. (b) Microcalorimetric titration of CAF with buffer (■), buffer with DAPI (●) and CAF with DAPI (▲) calculated as kcal/mol of titrant injected and plotted vs. total titrant concentration after correction for the temperature difference between the titrant and the sample cell. The approximate heat of DAPI–CAF interaction was calculated from the above data by subtracting the sum of the first two sets from the latter. The top three curves represent the extrapolation of experimental points to the value of $C_{TA}/C_{TC} \rightarrow 0$. The heat of CAF and DAPI dilutions were constant throughout the titration, and thus linear interpolation was made in this case (the heat of depolymerization of CAF is neglectible). Finally, the extrapolated heat of DAPI–CAF interaction was calculated by subtracting the sum of heats of dilutions from the heat of titration of CAF with DAPI (♦).

Ten aliquots of titrant (10 μl each) were added and the heat exchange (μcal/s) was measured as a function of time (Fig. 5a). The presented curves represent the titration of CAF with the buffer and CAF with DAPI. We measured titration of buffer with DAPI and buffer with buffer too (results not shown for clarity of the Fig. 5a) and all measured titrations were endothermic (Fig. 5b).

To estimate the enthalpy change of the DAPI–CAF interaction, we calculated measured heat exchanges as kcal/mol of titrant injected vs. titrant injected concentration (Fig. 5b). The approximate heat of the CAF–DAPI interaction can be extrapolated by subtracting the sum of heats of dilution (CAF with buffer and DAPI with buffer). From the intercepts of the extrapolation of the curve in Fig. 5b, the enthalpy change resulting from the interaction of CAF with DAPI was estimated to be $\Delta H = -11.1$ (± 0.4) kcal/mol.

5. Molecular modeling

The calculated stacking complex of DAPI with CAF is presented in Fig. 6. The lowest energy conformation is that in which CAF is oriented directly over the ring of DAPI with average face-to-face distance of 3.5 Å. Both molecules' rings are twisted with angle 70°. DAPI is a two-cation molecule, when we put it alone, without CAF, to periodic box with 42 molecules of water; it was bound with two molecules of them. CAF in the same conditions was also bound with two water molecules. But when we put DAPI and CAF to the same periodic boundary conditions, CAF 'lost' both bound water molecules. It confirmed the well-known fact that hydrophobic interactions are competitive to hydrophilic ones. The calculated enthalpy value resulting from the interaction of CAF with DAPI was estimated to be $\Delta H = -13$ kcal/mol. The details of molecular modeling calculations will be presented elsewhere.

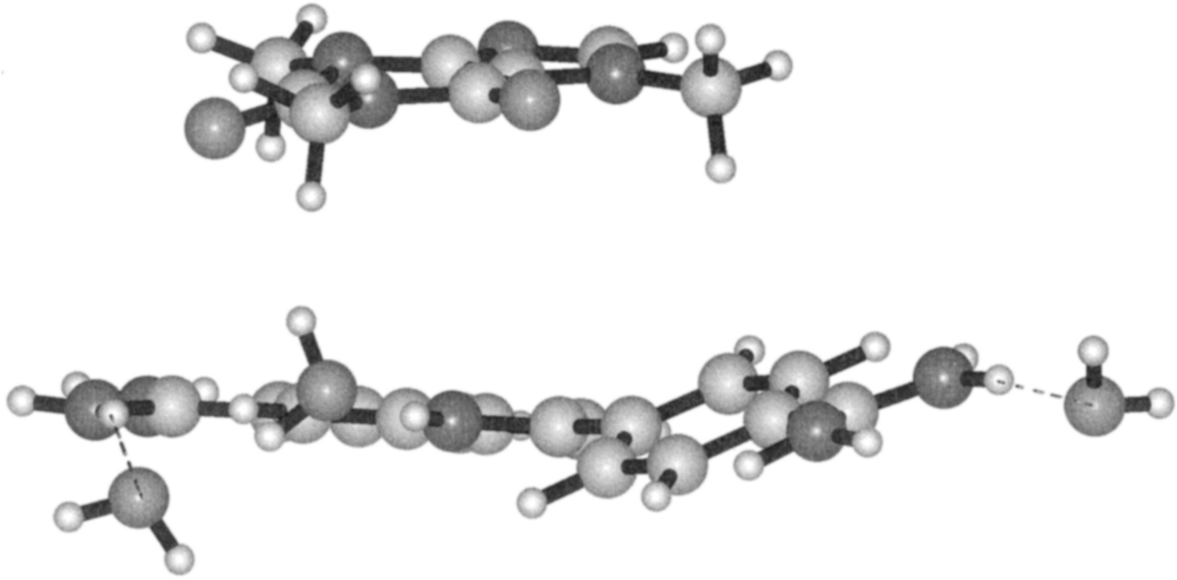

Fig. 6. Semi-empirical geometry optimization of the CAF–DAPI complex in the presence of 43 water molecules. All water molecules, with the exception of those which form hydrogen bonds (dotted lines) with DAPI, have been removed. For the clarity of the picture the double bonds have not been shown. The hydrogen atoms — small spheres, carbon — light gray, nitrogen — heavy gray, and oxygen atoms — medium gray spheres.

6. Conclusions

1. The light absorption studies provide evidence for stacking interactions between chosen ligands and CAF. The spectral shift in the absorption band of DAPI and EB in the presence of CAF is very characteristic for interactions between ligand chromophore and CAF; the shift was observed at > 350 nm, i.e. outside of the absorption of CAF.
2. Calculated values of mixed aggregation constants K_{AC} are in good agreement with values of stacking interaction constants [20,21].
3. The comparison of calculated and measured values of molecular concentrations proves the developed model is correct.
4. Observed effect of hyperchromicity of fluorescence spectra of ligands in the presence of CAF confirms stacking formation.
5. The titration microcalorimetric data provide additional information on the interaction between DAPI and CAF, the enthalpy of the reaction [-11.1 (± 0.4) kcal/mol] is consistent with stacking type of interaction [22–24].
6. The molecular modeling demonstrates that CAF can complex with the chosen ligands via stacking interaction.

Studies from several laboratories demonstrated that CAF is able to reduce the cytostatic and/or cytotoxic effect of DNA-intercalating agents. The present data indicate that this protective mechanism of CAF is a consequence of sequestration of such agents in stacking complexes with CAF, thus lowering the effective free ligand concentration in the solution and making the ligand less accessible.

Acknowledgements

We are grateful to Dr Maciej Zylicz for his helpful discussion. This work was supported by KBN 6 P203 044 06 and DS 0010-0002-4 grants.

References

[1] J. Labanowska, K.L. Beetham, L.J. Tolmach, Radiat. Res. 115 (1988) 176.
[2] H.J. Fingert, J.D. Chang, A.B. Pardee, Cancer Res. 46 (1986) 2463.
[3] J. Tanaka, B.A. Teicher, T.S. Herman, S.A. Holden, B. Dezube, E. Frei, Int. J. Cancer 48 (1991) 631.
[4] Y. Ohsaki, S. Ishida, T. Fujikane, K. Kikuchi, Oncology 53 (1996) 327.
[5] S. Fan, M.L. Smith, D.J. Rivet et al., Cancer Res. 55 (1995) 1649.
[6] K. Tomita, H. Tsuchiya, Jpn. J. Cancer Res. 80 (1989) 83.
[7] K.L. Beetham, P.M. Busse, L.J. Tolmach, J. Cell Physiol. 115 (1983) 283.
[8] F. Traganos, J. Kapuscinski, J. Gong, B. Ardelt, R.J. Darzynkiewicz, Z. Darzynkiewicz, Cancer Res. 53 (1993) 4613.
[9] F. Traganos, J. Kapuscinski, Z. Darzynkiewicz, Cancer Res. 51 (1991) 3682.
[10] H. Kimura, T. Aoyama, J Pharmacobiodyn. 12 (1989) 589.
[11] K. Weller, H. Schutz, I. Petri, Biophys. Chem. 19 (1984) 289.
[12] J. Kapuscinski, M. Kimmel, Biophys. Chem. 46 (1993) 153.
[13] J. Kapuscinski, Biotech. Histochem. 70 (1995) 220.
[14] J.-B. LePecq, C. Paoletti, J. Mol. Biol. 27 (1967) 87.
[15] B.C. Baguley, E.M. Falkenhaug, Nucleic Acids Res. 5 (1) (1978) 161.
[16] H.A. Crissman, M.S. Oka, J.A. Steinkamp, J. Histochem. Cytochem. 24 (1) (1976) 64.
[17] W. Thiel, Tetrahedron 44 (24) (1988) 7393.
[18] R.W. Larsen, R. Jasuja, R.K. Hetzler, P.T. Muraoka, V.G. Andrada, D.M. Jameson, Biophys. J. 70 (1996) 443.
[19] H. Fritzsche, I. Petri, H. Schutz, K. Weller, P. Sedmera, H. Lang, Biophys. Chem. 11 (1980) 109.
[20] W. Schimmack, H. Sapper, W. Lohmann, Biophys. Struct. Mech. 1 (1975) 311.
[21] J.-L. Dimicoli, C. Helene, JACS 95 (1973) 1036.
[22] S.J. Gill, M. Downing, G.F. Sheats, Biochemistry 6 (1967) 272.
[23] M.G. Marenchic, J.M. Sturtevant, J Phys. 77 (1973) 544.
[24] J. Sponer, H.A. Gabb, J. Leszczynski, P. Hobza, Biophys. J. 73 (1997) 76.